CIRRUS-HL: Overview of LIM contributions

Röttenbacher, J.[1,✉] **and Luebke, A. E.**[1,✉]
Müller H.[1], **Ehrlich, A.**[1], **Schäfer, M.**[1], **Kirbus B.**[1], **Wendisch, M.**[1]

[1] *Leipzig Institute for Meteorology, Universität Leipzig, Leipzig, Germany*
✉*e-mail: johannes.roettenbacher@uni-leipzig.de, anna.luebke@uni-leipzig.de*

Summary: From June to July 2021, the Leipzig Institute for Meteorology (LIM) participated in the Cirrus in High Latitudes (CIRRUS-HL) campaign. Utilizing the German High Altitude Long Range Research Aircraft (HALO), 24 research flights were conducted out of Oberpfaffenhofen, Germany. The initial goal of the campaign was to sample high-latitude cirrus clouds with a combination of in-situ and remote sensing instrumentation. However, due to the global coronavirus pandemic, the flights had to be carried out from southern Germany instead of northern Sweden. Thus, the flight time in Arctic latitudes was limited. Therefore, more objectives concerning midlatitude cirrus were included in the campaign goals. LIM contributed to CIRRUS-HL with measurements by the Broadband AirCrAft RaDiometer Instrumentation (BACARDI) and the Spectral Modular Airborne Radiation measurement sysTem (SMART). While BACARDI measured broadband solar and terrestrial upward and downward irradiance, SMART measured spectrally resolved solar upward radiance as well as upward and downward irradiance.

Zusammenfassung: Von Juni bis Juli 2021 nahmen einige Mitarbeitende des LIM an der CIRRUS-HL Kampagne teil. Mit dem deutschen Forschungsflugzeug HALO (High Altitude Long Range Research Aircraft) wurden 24 Forschungsflüge von Oberpfaffenhofen, Deutschland, aus durchgeführt. Ursprüngliches Ziel der Kampagne war es, Zirruswolken in hohen Breitengraden mit einer Kombination aus In-situ- und Fernerkundungsinstrumenten zu untersuchen. Aufgrund der weltweiten Corona-Pandemie mussten die Flüge jedoch von Süddeutschland statt von Nordschweden aus durchgeführt werden. Daher wurden weitere Ziele in Bezug auf Zirruswolken in mittleren Breiten in die Ziele der Kampagne aufgenommen. Das LIM-Team betrieb die breitbandigen und spektralen Strahlungssensoren BACARDI (Broadband AirCrAft RaDiometer Instrumentation) und SMART (Spectral Modular Airborne Radiation measurement sysTem), wobei BACARDI die breitbandige solare und terrestrische Auf- und Abwärtsstrahlung und SMART die spektral aufgelöste solare Auf- und Abwärtsstrahlung sowie die Aufwärtsstrahlungsdichte maß.

1 Introduction

The impact of cirrus clouds on our current and changing climate is a critical point for comprehending the Earth's climate system. In particular, cirrus clouds in the Arctic present a key uncertainty of the Arctic energy budget as it might switch from a warming to a cooling effect depending on the changing properties of clouds moving between ocean and ice covered surfaces and the sensitivity of the larger climate system to perturbations. Midlatitude cirrus clouds were studied with the German High Altitude Long Range Research Aircraft (HALO) in the MidLatitude Cirrus (ML-CIRRUS) airborne campaign in 2014. Building onto that successful mission and the established extensive instrument payload, the CIRRUS-HL campaign was carried out in June and July 2021 to probe Arctic cirrus clouds. The scope of the mission is to study formation, properties, and climate impacts of cirrus clouds in high latitudes, compare them to midlatitude cirrus and investigate the aviation impact on cirrus. The main objectives were to quantify ice crystal properties, the impact of the aerosol particles and the radiative effects of cirrus clouds.

Due to the impact of the ongoing coronavirus pandemic on the logistics of the campaign, the original spring time frame for the campaign and measurements based out of Kiruna, Sweden, could not be realized. Instead, the campaign was shifted to Oberpfaffenhofen, Germany, and moved to the summer. This compelled the scientists to reevaluate their flight strategies, and the major goals of the mission could still be achieved while incorporating further research objectives.

A team of scientists from the Leipzig Institute for Meteorology (LIM) participated in this study with two remote sensing packages on board. The following sections provide more details on the goals of the campaign, an overview of the campaign results, information on the instruments operated by LIM and a case study demonstrating how the measurements from these instruments can be used for future analyses.

2 Campaign overview and instrumentation

The CIRRUS-HL campaign resulted in 24 measurement flights with a total of 146 flight hours. Figure 1 illustrates an overview of the flight tracks from the campaign. In order to accommodate more time spent measuring in the Arctic, several flight days included double flights, wherein HALO would refuel in the Arctic to extend the measurement time in high latitudes. However, HALO also took advantage of its home base in Oberpfaffenhofen and managed to also fly in midlatitude cirrus systems and obtain measurements collocated with ground-based stations across Germany in Jülich, Leipzig, Munich and Lindenberg.

The research flights were designed to follow one or more of the seven objectives of CIRRUS-HL, which comprise Arctic in-situ cirrus in ice supersaturated regions (ISSR), Arctic frontal cirrus, midlatitude in-situ cirrus, midlatitude frontal cirrus, embedded contrails in cirrus, contrail cirrus hotspots and exemplary cases of cirrus influenced by soot.

The LIM team operated two passive radiation sensors on board HALO. Both instruments are described in the following subsections, and for reference, their respective

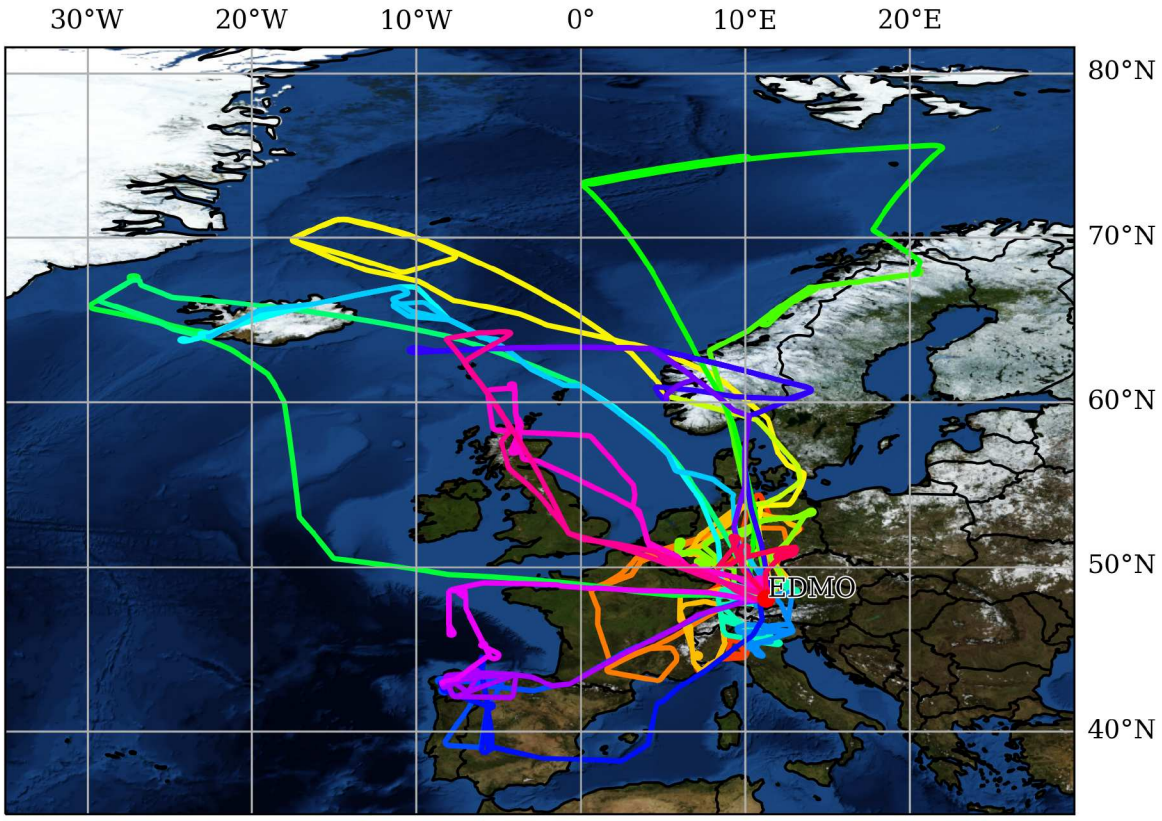

Figure 1: *Flight tracks from all 24 research flights during CIRRUS-HL (background: NASA Visible Earth).*

positions on the aircraft can be seen in Fig. 2. In addition, Table 1 provides an overview of both instruments and key specifications.

Figure 2: *HALO during landing with the locations of the different radiation sensors. Photo: Andreas Minikin; Instrument photos: Roger Riedel, Hanno Müller.*

Table 1: *Overview of instrument specifications.*

Instrument	**Time resolution**	**FOV**	**Wavelength range**	**Vertical resolution**	**Measured quantity**	**Derived/retrieved parameters**
BACARDI	0.1 s	180°	0.2 – 3.6 µm (pyranometer); 4.5 – 42 µm (pyrgeometer)	integrated	Up- and downward broadband solar and terrestrial irradiance	Albedo, net irradiance, heating rate profiles
SMART	0.3 s	180°, 2° (radiance)	0.3 – 2.2 µm	integrated	Up- and downward spectral irradiance, upward spectral radiance	Cloud top reflectivity, spectral net irradiance, albedo

2.1 Overview of instrumentation

The majority of the instrumentation on board HALO for the CIRRUS-HL campaign is designed for in-situ measurements (Voigt et al., 2017). Thirteen in-situ instruments with inlets on the fuselage of the aircraft were installed to measure water vapor, water content and different aerosols. Eight more cloud probe instruments employing various measurement techniques were installed along the wings of HALO. These cloud probes provide valuable information concerning cloud particle number concentrations and images of cloud particles to determine particle sizes and shapes. In addition to the remote sensing instruments operated by LIM, the WALES lidar (name derived from WAter vapor Lidar Experiment in Space; Wirth et al., 2009) and the spectral imager (specMACS; Ewald et al., 2016) were also part of the payload. A schematic overview is shown in Fig. 3 where a) shows the instruments located inside the aircraft with inlets or windows on the fuselage of HALO and b) shows the particle and in-situ probes mounted on the wings of HALO. A more detailed description of each instrument is given on the campaign website https://cirrus-hl.de/instruments.

2.2 BACARDI

The radiometer package on HALO, the Broadband AirCrAft RaDiometer Instrumentation (BACARDI), consists of two sets of Kipp and Zonen pyranometers (CMP 22) and pyrgeometers (CGR-4) mounted to the fuselage of the aircraft. The upward and downward solar ($0.2 - 3.6\,\mu m$) and terrestrial ($4.5 - 42\,\mu m$) irradiances at flight level are measured using this configuration of four radiometers. Based on these measurements, the radiative forcing of cirrus clouds can be calculated with the help of radiative transfer simulations. Because the instruments measure the irradiance of the full sky, including cloudy and cloud-free areas, simulations are performed using the libRadtran package (Emde et al., 2016) to calculate the irradiance of the cloud-free case in order to isolate cloud radiative effects alone (Luebke et al., 2022). A more detailed description of the instrument as well as the measurement uncertainties and post-processing are provided in Luebke et al. (2022). Postprocessed data from the BACARDI instrument for the CIRRUS-HL campaign are published on the HALO Database (https://halo-db.pa.op.dlr.de/).

2.3 SMART

During CIRRUS-HL, the Spectral Modular Airborne Radiation measurement sysTem (SMART; Wolf et al., 2019) measured downward and upward irradiance as well as upward nadir radiance in the spectral range between 0.3 µm and 2.2 µm. The spectral resolution (Full Width at Half Maximum (FWHM)) of the instrument is $2 - 3$ nm for wavelengths below 1.0 µm and 10 –15 nm for longer wavelengths. The integration time was set to 300 ms resulting in a temporal resolution of 3.3 Hz. The radiance sensor has a field of view of $2\,^\circ$, which together with the temporal resolution results in a footprint of approximately $422\,m \times 349\,m$, assuming an aircraft speed of $220\,m\,s^{-1}$ and an altitude of 10 km. Notably, the optical inlet for the downward irradiance is mounted to a leveling platform to actively maintain a horizontal position. The two inlets for upward irradiance and radiance were mounted in a fixed position. With this setup, the spectrally resolved solar radiative budget at flight altitude was derived.

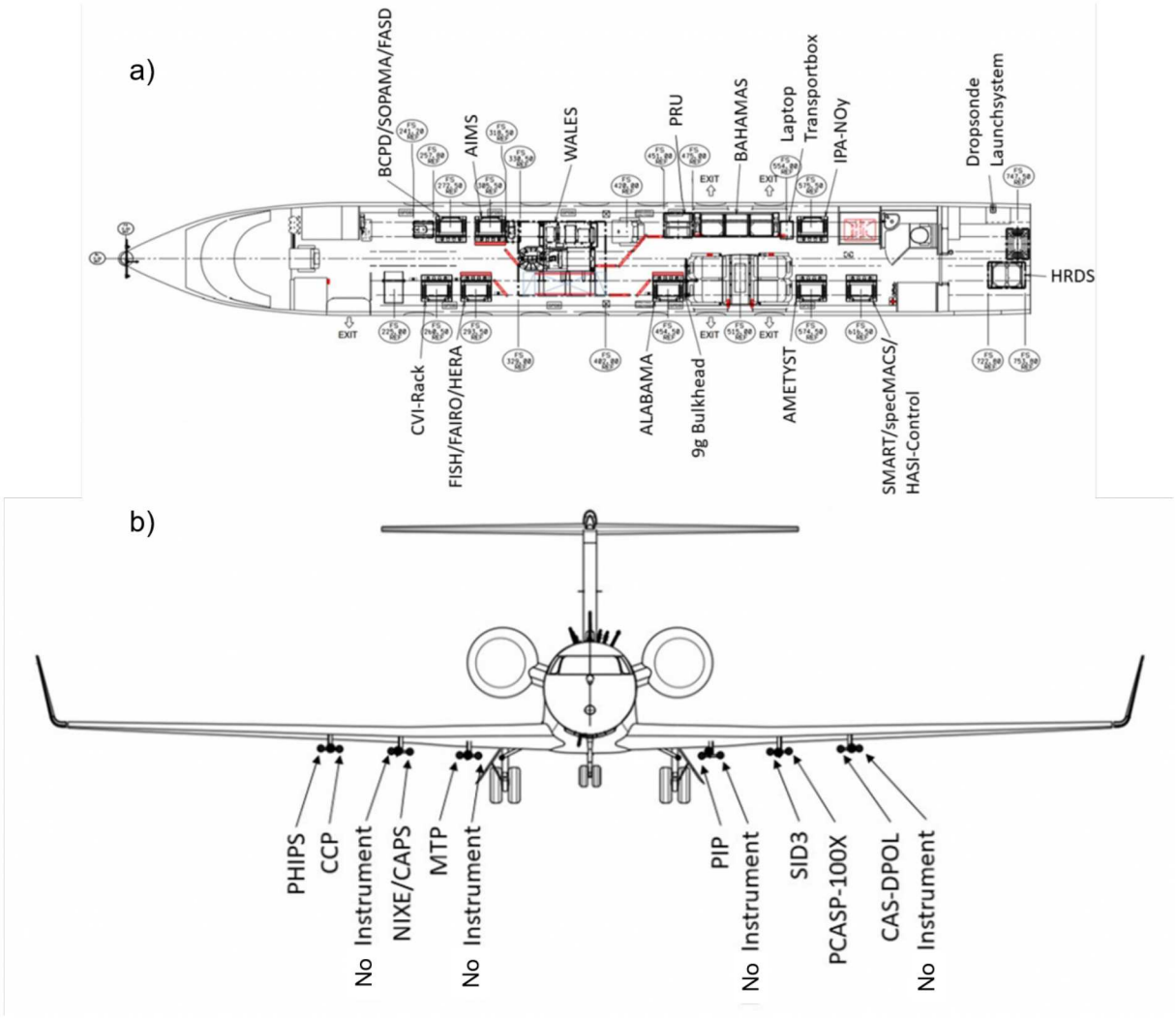

Figure 3: *Schematic depicting the position of measurement instruments a) on board HALO and b) attached to the wings during the CIRRUS-HL campaign. See https://cirrus-hl.de/instruments for details on the abbreviations and instruments.*

3 Case study of measurements

To demonstrate how the observations of the SMART and BACARDI instruments are used to study cirrus cloud radiative effects, a case study from the double flight on 29 June 2021 is used, which comprises Research Flights (RF) 05 and 06. However, we consider only RF05 here. The overall goal of this particular flight was to sample an Arctic cirrus system just east of Greenland and north of Iceland, which could be accommodated by a refueling stop in Bergen, Norway at the end of RF05. The synoptic conditions east of Greenland were dominated by a strong high pressure ridge located between Iceland and Scandinavia. This caused a southwesterly flow, lifting an air mass east of Greenland and forming a warm front. Cirrus clouds formed along the associated ridge. An in-situ, Lagrangian, staircase flight pattern was chosen to probe this system over the course of approximately 2 hours. With this strategy, different vertical layers of the cirrus system could be observed. The flight track with the different sections of the staircase pattern and an impression of the cloud field can be seen in Fig. 4.

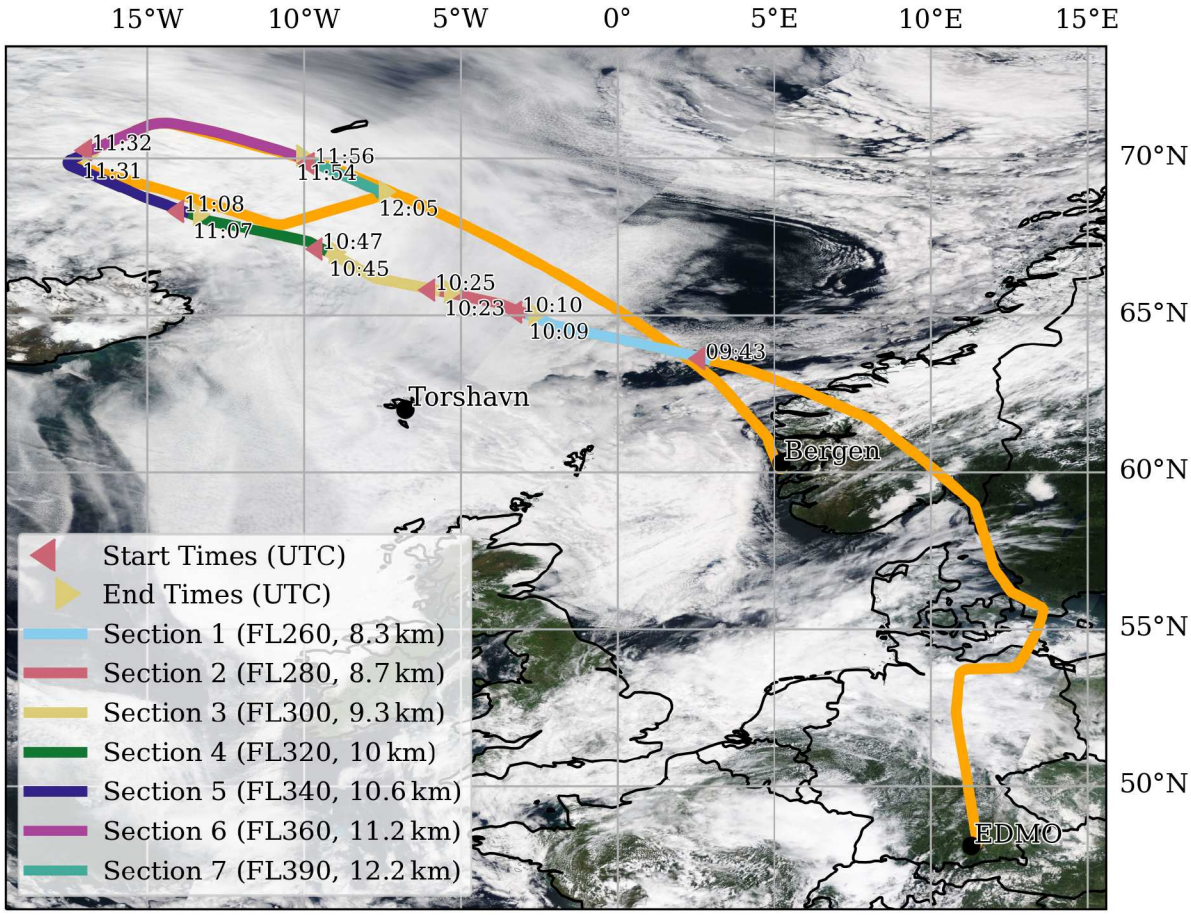

Figure 4: *HALO flight track of RF05 on 29 June 2021 starting from Oberpfaffenhofen (EDMO) towards the north of Iceland. Colors depict the position of HALO according to the sections defined by altitude. The satellite image is the corrected reflectance from the MODIS instrument on board Terra retrieved on 29 June 2021.*

The staircase pattern started at FL260, which was below the cirrus cloud deck. A cloud-free atmosphere was observed under HALO at this time. The aircraft first ascended into a thin cirrus cloud layer. As HALO continued to climb, the aircraft was persistently in clouds until FL320, where the cirrus cloud became more patchy. Some thicker cirrus cloud was encountered, but became thinner and intermittent at FL360. At FL390, HALO completed the pattern and was above the cirrus cloud layer.

3.1 BACARDI

Figure 5 provides time series of observed and simulated upward and downward, solar and terrestrial irradiance, respectively, throughout RF05. The simulations, which represent the cloud-free case, are shown as a reference. The points where the simulations and observations match indicate flight sections with cloud-free observations of either the upward or downward irradiance. From Fig. 5, it is clear that large sections of the flight were in cloudy conditions. Although the irradiance observations can be used to infer the cloud situation, additional observations of the clouds above or below the aircraft provide necessary contextual information. Thus, the following interpretations of the data are subject to some uncertainty and require further analysis for confirmation.

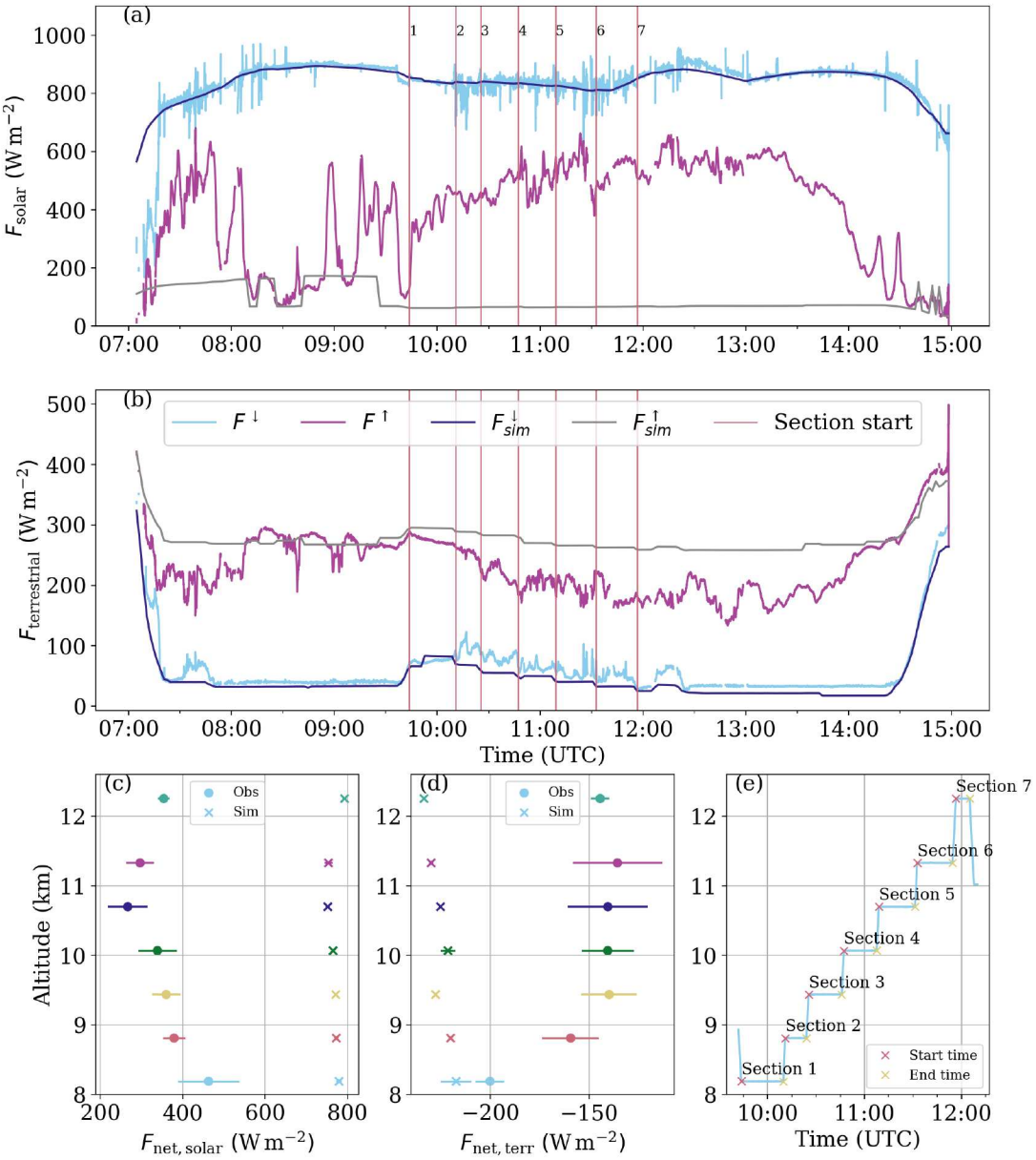

Figure 5: *BACARDI observations from RF05 on 29.06.2021. (a) and (b) depict time series of solar and terrestrial irradiance observations and cloud-free simulations, respectively, for the whole flight. (c) and (d) show the observed and simulated mean net solar and terrestrial irradiance for each flight section during the staircase flight pattern. Bars indicate the standard deviation for each level. (e) illustrates the different altitude sections over the same time period for reference.*

Figure 5 (c) and (d) depict the mean net irradiance (F_{net}) for each of the sections during the in-situ, Langrangian staircase sequence. Simulations of F_{net} for the cloud-free case are also shown for reference. In general, the observed net solar irradiance ($F_{\text{net,solar}}$) is decreasing with altitude. This is due to the fact that with higher altitude, the cloud layer below HALO becomes thicker and increases the reflection of solar irradiance. The cloud layer above becomes thinner and transmits more incoming solar irradiance. In this case, we see that the upward solar irradiance is increasing while the downward component remains relatively stable, even as the aircraft moves into and under cirrus cloud layers.

In Flight Section 5, just below 11 km, there is a sharper decrease in $F_{\text{net,solar}}$. The cirrus clouds in this section were reported to first become thicker, which increases the amount of solar radiation being reflected by the lower clouds and reduces the transmitted solar radiation, thus decreasing $F_{\text{net,solar}}$. However, $F_{\text{net,solar}}$ increases again as the aircraft exits this layer into thin, intermittent clouds, where the upward solar irradiance could be less intense, however confirmation of this assumption depends on the cloud situation below HALO. The fact that the simulated $F_{\text{net,solar}}$ is much higher than the observations suggests that there is also a stratitform cloud layer at lower altitudes, which increases the upward solar irradiance relative to a case where there are no clouds below HALO. This stratus cloud layer is likely to also be changing and affecting the upward irradiance.

In the terrestrial net irradiance ($F_{\text{net,terr}}$), the profile in Fig. 5(d) first increases sharply with altitude, but then stabilizes around 10 km (Flight Section 4). In the lower altitudes of the profile (Flight Sections 1–3), Fig. 5(b) shows that the downward terrestrial irradiance is not decreasing as rapidly as the upward component. This coincides with HALO entering the base of the cirrus cloud. The upward irradiance decreases due to the emission of terrestrial radiation by the cirrus cloud layer, which is colder than the surface. The emitted downward terrestrial irradiance only decreases slowly as the cloud base temperature is only slightly warmer than the temperature of the higher cirrus cloud layers. In the higher part of the profile (Flight Sections 4–7), the upward terrestrial irradiance continues to decrease with altitude, but the cirrus cloud is reported to be more intermittent and thin, with only some denser samples. Thus, the upward terrestrial irradiance decreases more slowly than at the lower altitudes of the profile. At the same time, the cold atmosphere above the cirrus cloud layer continues to impact the downward terrestrial irradiance, particularly as HALO nears the top of the layer. Both effects compensate for each other and stabilize $F_{\text{net,terr}}$ until Flight Section 7, when HALO is above the clouds completely, and the magnitude of the cooling increases ($F_{\text{net,terr}}$ decreases).

Similar to the $F_{\text{net,solar}}$ profile around 11 km, $F_{\text{net,terr}}$ is also affected by the very dense cirrus cloud layer and transition to patchier, thinner cirrus clouds. This is not obvious in the mean $F_{\text{net,terr}}$, but is indicated by the larger standard deviation bars in Flight Sections 5 and 6, where it is demonstrated that the terrestrial fluxes are fluctuating as the density of the cloud within and between layers changes too. In the case of both $F_{\text{net,solar}}$ and $F_{\text{net,terr}}$, additional information about the microphysical and macrophysical properties of the cloud can help to more clearly interpret the observations.

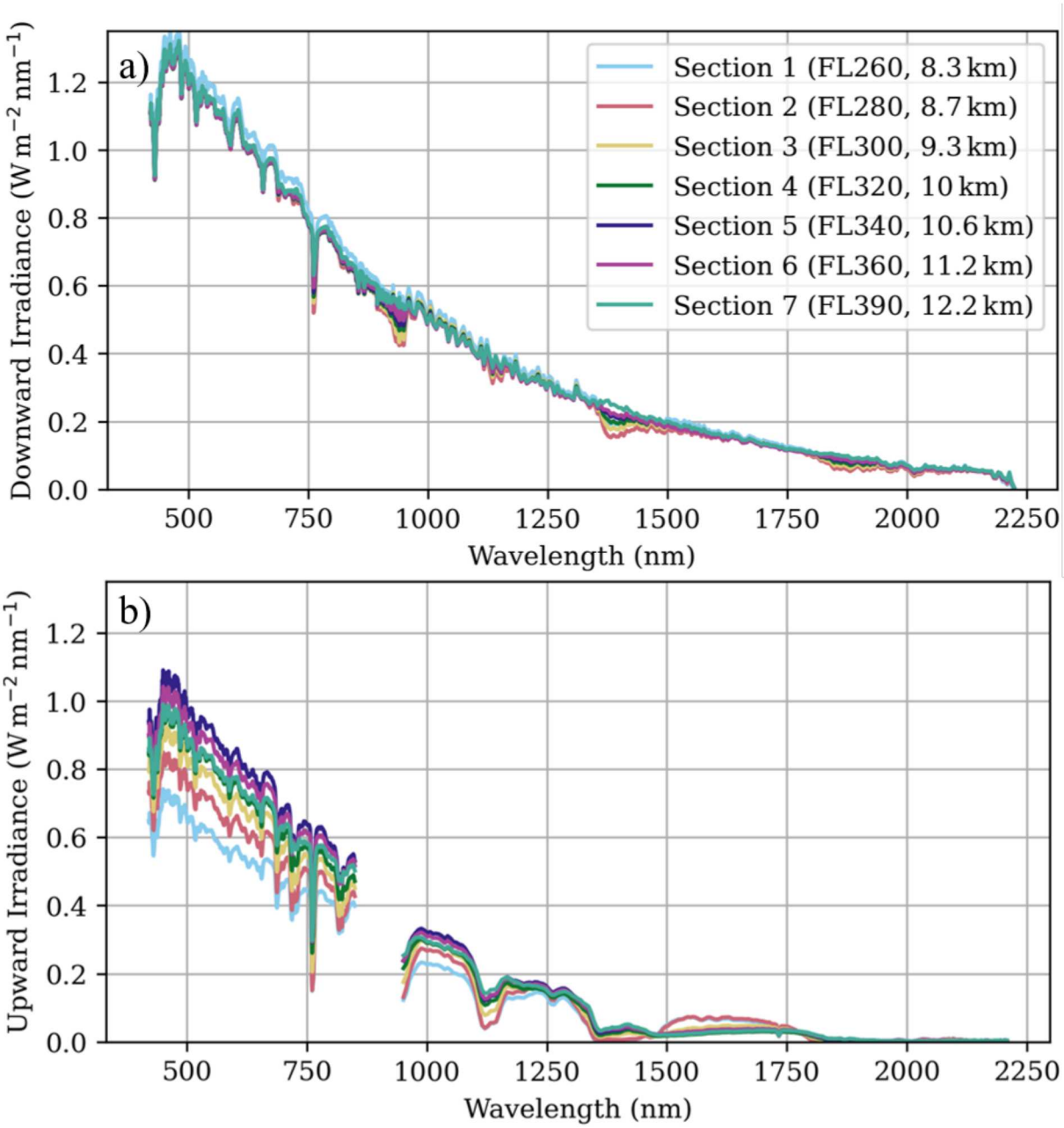

Figure 6: *Average SMART spectra for each section of the staircase pattern, (a) downward irradiance, (b) upward irradiance.*

3.2 SMART

The broadband measurements by BACARDI were complemented by spectral information provided by the irradiance measured with SMART in the solar part of the spectrum from 0.3 nm – 2200 nm. The spectral information allows for conclusions to be made on the cirrus cloud microphysical properties and their representation in radiative transfer models.

Figure 6 shows the average spectral downward irradiance (a) and upward irradiance (b) for each section of the staircase pattern. The variability of the downward irradiance indicates the presence/absence of cirrus clouds above HALO but is also is caused by the changing solar zenith angle. Flight Section 1 shows the highest values because it

includes parts with no cloud above and is located further south with a lower solar zenith angle than Section 7, which is exclusively above cloud. Apart from this, the different sections do not show significant differences in most of the spectrum. This shows that the extinction by the optically thin cirrus cloud does not attenuate the incoming solar radiation significantly. However, in particular wavelength ranges absorption by atmospheric trace gases is obvious.

The first notable absorption line at 760 nm corresponds to an oxygen absorption line, which becomes more pronounced the lower the altitude of HALO. Three broader sections can be identified at around 900 nm, 1350 nm and 1850 nm. They all correspond to water vapour absorption bands with centers at 940 nm, 1380 nm and 1870 nm. With increasing altitude and thus less cirrus cloud above the aircraft, the dip in the spectrum gets less pronounced. This can be explained by the decrease in the absolute amount of water vapour above the aircraft, which directly correlates with the amount of cirrus clouds. In addition, the path a photon needs to travel decreases with increasing altitude, thus decreasing the chance of it being absorbed inside the cirrus clouds.

The upward irradiance in Fig. 6(b) shows a higher variability between the different sections. Different processes lead to the change of the upward irradiance, which does not follow a steady increase with altitudes as would be the case for a homogeneous cirrus cloud. In this case, a lower stratiform cloud layer increased the reflectivity from altitudes below the cirrus cloud. As the cloud optical thickness of this stratiform cloud might change along the flight track, the upward irradiance becomes variable. In the wavelength range between 1500 and 1700 nm, the absorption by cloud particles dominates the spectral pattern. For the high flight section, when HALO is above the cirrus clouds, the upward irradiance is reduced compared to lower altitudes. This indicates the absorption by ice crystals and the presence of cirrus clouds. In this spectral range, the large ice crystals of the cirrus cloud absorb solar radiation more strongly than the small liquid droplets of the low stratiform cloud. To disentangle the different effects and quantify the radiative effect of the cirrus cloud, a sensitivity study using radiative transfer simulations is required.

4 Conclusions and outlook

CIRRUS-HL provides a new data set for analyzing the microphysical and radiative properties of Arctic and midlatitude cirrus clouds. Here, spectral and broadband irradiance measurements by BACARDI and SMART are presented for an Arctic cirrus cloud north of Iceland. The irradiances reveal the complexity of this case, which was caused by a low level liquid cloud layer and the heterogeneity of the cirrus cloud. Comparison with radiative transfer simulation of cloud-free conditions with profiles of up- and downward irradiance illustrate the solar radiative effect by the cirrus cloud, which is often superimposed by the reflection of radiation by the lower stratiform cloud. In the terrestrial wavelength range, the effect of the low cloud is less important. This illustrates, that different spectral ranges need to be analysed to separate the radiative effects of both cloud layers. Similarly, the spectrally resolved measurements of SMART can be used in combination with radiative transfer simulations to extract the radiative effects of ice crystals. To interpret the radiation measurements, the full HALO instrumentation of CIRRUS-HL can be used to combine remote sensing measurements with in-situ measurements of

ice particle size, shape and number. By constraining the influence of the lower-cloud albedo with model analyses, these data can be used to assess the impact of ice crystal properties, such as ice crystal shape, on the radiative effect of Arctic cirrus clouds. It is envisioned to compare the CIRRUS-HL observations with numerical weather forecast models and cirrus cases observed in the central Arctic during the recent HALO campaign HALO-(AC)³.

References

Emde, C., Buras-Schnell, R., Kylling, A., et al.: The libRadtran software package for radiative transfer calculations (version 2.0.1), Geosci. Model Dev., 9, 1647–1672, doi:10.5194/gmd-9-1647-2016, 2016.

Ewald, F., Kölling, T., Baumgartner, A., Zinner, T., and Mayer, B.: Design and characterization of specMACS, a multipurpose hyperspectral cloud and sky imager, Atmos. Meas. Tech., 9, 2015–2042, doi:10.5194/amt-9-2015-2016, 2016.

Luebke, A. E., Ehrlich, A., Schäfer, M., Wolf, K., and Wendisch, M.: An assessment of macrophysical and microphysical cloud properties driving radiative forcing of shallow trade-wind clouds, Atmospheric Chemistry and Physics, 22, 2727–2744, doi:10.5194/acp-22-2727-2022, 2022.

Voigt, C., Schumann, U., Minikin, A., et al.: ML-CIRRUS: The Airborne Experiment on Natural Cirrus and Contrail Cirrus with the High-Altitude Long-Range Research Aircraft HALO, Bull. Amer. Meteor. Soc., 98, 271–288, doi:10.1175/BAMS-D-15-00213.1, 2017.

Wirth, M., Fix, A., Mahnke, P., et al.: The airborne multi-wavelength water vapor differential absorption lidar WALES: system design and performance, App. Phys. B, 96, doi:10.1007/s00340-009-3365-7, 2009.

Wolf, K., Ehrlich, A., Jacob, M., et al.: Improvement of airborne retrievals of cloud droplet number concentration of trade wind cumulus using a synergetic approach, Atmospheric Measurement Techniques, 12, 1635–1658, doi:10.5194/amt-12-1635-2019, 2019.